

Image Analysis of Radial Symmetrical Samples

PETR PONÍŽIL¹, VLADIMÍR PAVLÍNEK², TAKESHI KITANO², TOMÁŠ DŘÍMAL³

¹Faculty of Technology,

²Polymer Centre,

³Faculty of Applied Informatics,

Tomas Bata University in Zlin,

TGM 275, 762 72 Zlin,

CZECH REPUBLIC

<http://fyzika.ft.utb.cz/personal/petr/>

Abstract: A method of image analysis of images, which are developed from electrorheological samples, is presented. Due to the process of preparation, electrorheological samples show a radial symmetry. Numerical transformations are necessary to remove sample deformation and obtain correct radial dependence of image intensity as the function characterizing the sample image.

Key-Words: Image analysis, radial symmetry

1 Introduction

Electrorheological (ER) fluids are systems whose rheological properties (viscosity, yield stress, shear modulus) can be controlled by external electric field. For the fluids researched so far, ER effect usually causes a continuous increase in viscosity, or immediate (in milliseconds) solidification of the material. This is called a positive electrorheological effect. However, also the opposite effect has been described for several systems – a decrease of viscosity in electric field (a negative ER effect). These facts indicate a wide range of possible practical applications, therefore understanding of the phenomena is highly desirable.

The positive ER effect, which was described by Winslow (1) more than 50 years ago, has been in focus of many papers concentrating on the elucidation of the mechanism, preparation of ER fluids with optimum efficiency and their possible use. The research findings can be found in a number of comprehensive reviews (2–4).

Majority of electrorheological fluids are suspensions of solid particles in electrically non-conducting fluid (usually mineral or vegetable oils). First dispersed phase was represented by inorganic or organic materials, water-free or with some portion of water or other activators. Recent generations of ER fluids are based on suspensions of electrically conducting polymers and nanoparticles of various nature, because of their suitable polarizability.

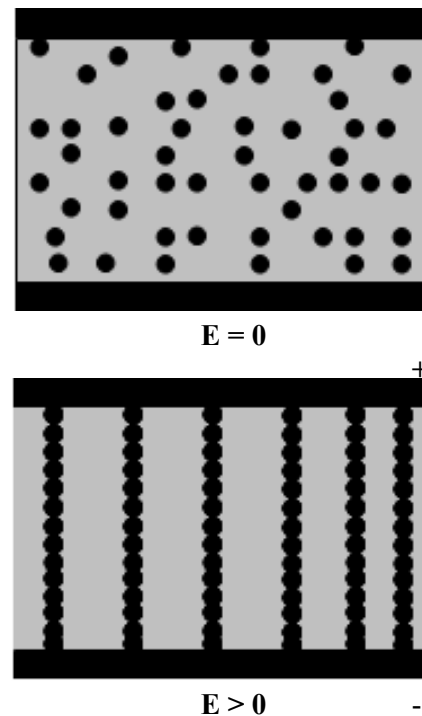


Fig. 1: Scheme of chain structure of ER suspension without flow field.

ER effect is considered to be caused by interfacial polarization of dispersed particles (3,4) produced by external DC or AC electric fields of high intensity (E in order of kV/mm). Polarized particles are oriented in the direction of electric field and create structures (chains), which increase the rigidity of the originally liquid system (Fig. 1). On the application of flow field, at low shear rates viscosity is high (after exceeding possible yield stress). It is supposed that shear forces cause degradation of the structures created; therefore

viscosity falls with a rise of shear rate and finally, at high shear rates, it gets to the level of zero-field viscosity.

The arrangement of the particle chains in electric field has been proved via optical microscopy. In order to explain the mechanism of reorganization of these structures in electric field during flow, majority of studies so far have followed the dependence of rheological and viscoelastic behaviour (gradient dependence of viscosity, shear stress, viscoelastic moduli) or yield stress of ER fluids in relation to the chemical nature, and physical properties of dispersed particles which affect their polarizability (particle size and shape, DC and AC electric conductivity, permittivity and dielectric loss). However, these results do not provide any evidence of the changes in particle arrangement during flow. On the other hand, direct optical display of ER suspensions in rotational viscometer presented in papers (5,6) indicated that particles organize into lamellar or ring structures, which are optimal for minimum energy dissipation, and this structure depends on the flow field (Fig. 2). These experiments, which have only been carried out for several systems, showed the way to the elucidation of general factors controlling flow mechanism of ER structures.

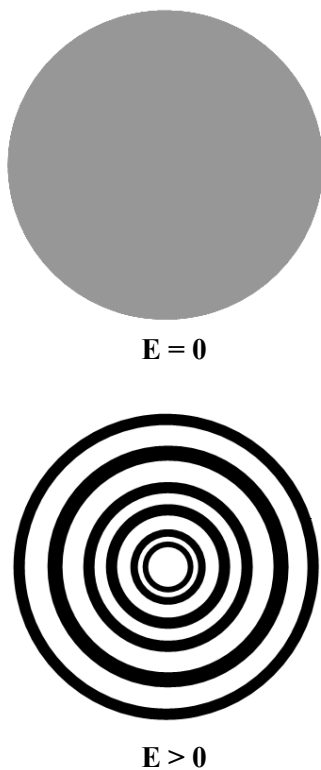


Fig. 2: Example of a structure of electrorheological suspension formed between two rotating parallel plates

2 Experiment

2.1 Centring

Samples were scanned on commercial scanner and greyscale images as Fig. 3 with typical size 1000x1000 pixels were obtained. The goal is to gain radial dependence of darkness of the image. Suppose that $p(x,y)$ is brightness of pixel in x -column and y -row of the image.

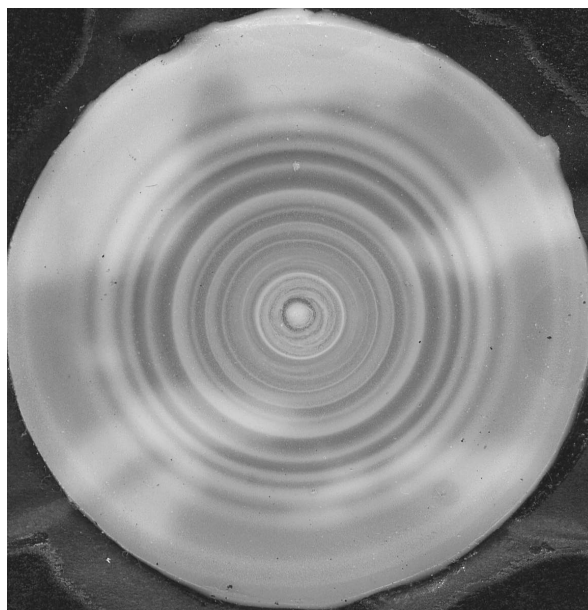


Fig. 3: The scanned image of electrorheological sample.

There are several problems. Samples are relatively soft and easy deformable. The images are a little prolonged in some directions.

The first task is to recognize position of centre of symmetry. The first estimation of the centre position (x_{c0}, y_{c0}) can be made manually or automatically (as the centre of the image). For some neighbourhood a symmetry function $S(x_c, y_c)$ is computed as

$$S(x_c, y_c) = \sum_{x,y=-200}^{200} \frac{(p(x_c + x, y_c + y) - p(x_c - x, y_c - y))^2}{\sqrt{x^2 + y^2}}$$

where numerator is square of brightness difference of symmetrical pixels and denominator is weight (number of pixels in some distance is proportional to this distance). Fig. 4 shows graphical representation of $S(x_c, y_c)$ function. Brighter pixels indicate higher value of $S(x_c, y_c)$ function, cross near image centre indicates position of real symmetry centre – the total maximum of $S(x_c, y_c)$ function with position (x_{cm}, y_{cm}) .

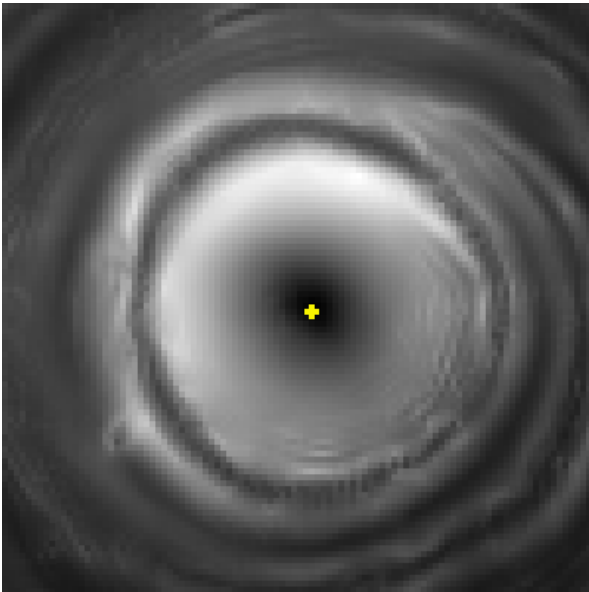


Fig. 4: The graphical representation of $S(x_c, y_c)$ function.

2.2 Transformation

If the centre is found, image is divided into 8 radial sectors and mean brightness as a function $f_i(r)$ (index i denotes the sector) of the real centre distance r is computed. On the fig. 5 is the comparison of such functions for two different sectors of image. It is obvious that a little shift and scale change is necessary to eliminate deformation.

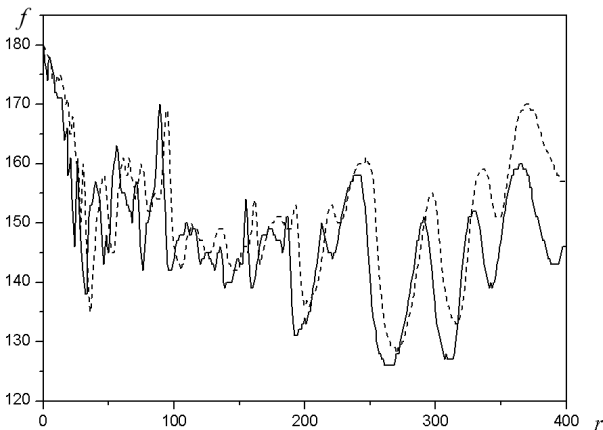


Fig. 5: The comparison of $f_i(r)$ functions for two sectors. Intensity f and radial distance r are both in arbitrary units.

A tool for the examination of the similarity of two functions is cross-correlation function (7,8). This function is defined for real functions as

$$(f_i * f_j)(x) = \int f_i(r) f_j(r + x) dr .$$

For example, consider two real valued functions f_i and f_j that differ only by a shift along the x -axis. One can calculate the cross-correlation to figure out how much f_j must be shifted along the x -axis to make it identical to f_i . The formula essentially slides the f_j function along the x -axis, calculating the integral for each possible amount of sliding. When the functions match, the value of $(f_i * f_j)$ is maximized. The reason for this is that when lumps (positives areas) are aligned, they contribute to making the integral larger. Also, when the troughs (negative areas) align, they also make a positive contribution to the integral because the product of two negative numbers is positive. For our occasion we define cross-correlation function more generally as

$$(f_i * f_j)(h, x) = \int f_i(r) f_j(hr + x) dr ,$$

where h is a scale change and x is a shift. If the value of $(f_i * f_j)$ is maximized, the best combination of h and x is found (9).

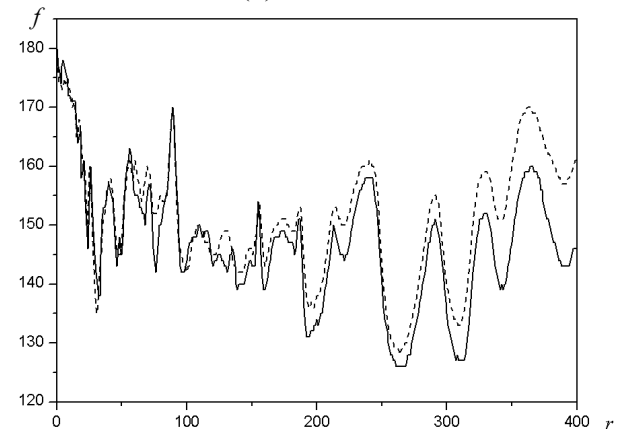


Fig. 6: The original $f_i(r)$ function and transformed $f_2(hr+x)$ function. Values $h = 0.972$, $x = -5.07$ maximize the cross-correlation function.

2.3 Results

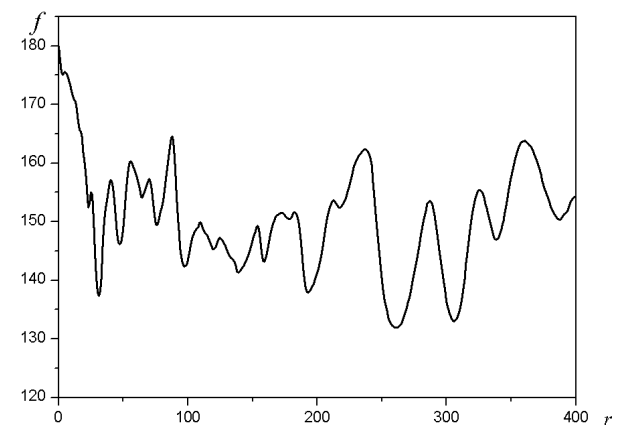


Fig. 7: The averaged $f(r)$ function.

After rescaling of f_j functions for each sector, the mean value of one original and all transformed f_j functions is computed. This way was obtained the average $f(r)$ function as the dependence of average intensity on radial distance from sample centre and is presented on the Fig. 7.

Fig. 8 shows comparison of the central part of the original sample image and corresponding image based on radial dependence of intensity $f(r)$ from Fig. 7.

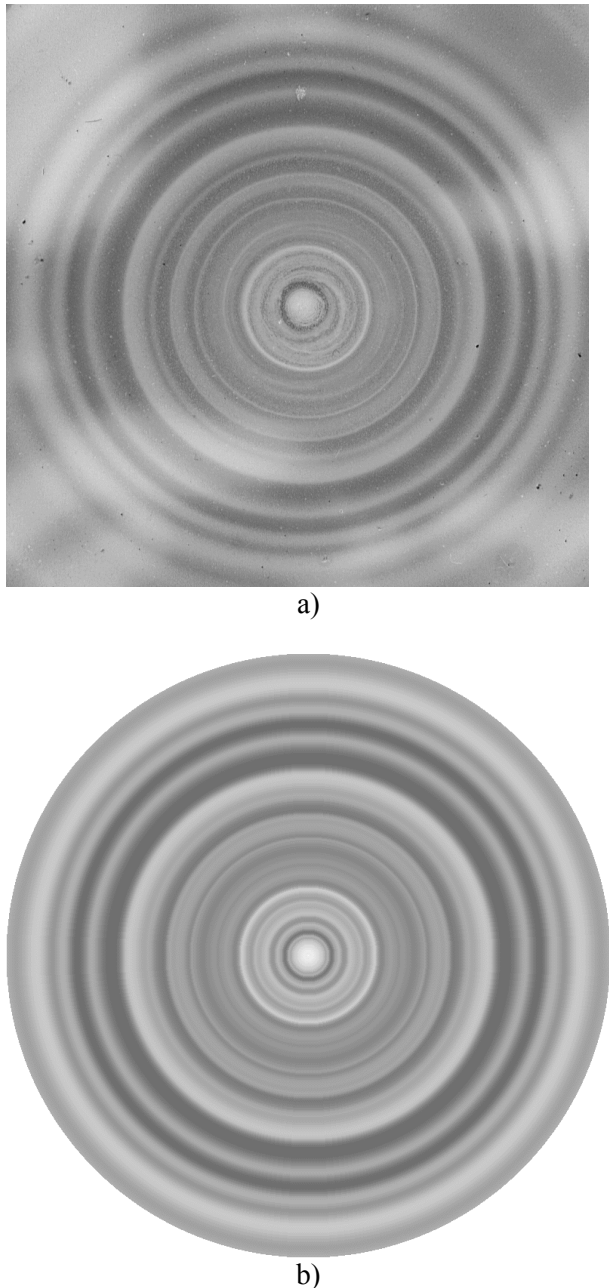


Fig. 8: The central part of the original image (a) and corresponding result of the image optimization (b).

Now the sample is characterized by the $f(r)$ function as showed on Fig. 7. A dependence of distribution of peaks of the $f(r)$ function on parameters of samples preparation can be studied.

3 Conclusion

A method of the optimization of radial symmetrical images was suggested.

Acknowledgements

The authors kindly acknowledge the support by the Ministry of Education, Youth and Sport of the CR (project MSM 7088352101), the Czech Science Foundation (projects 106/05/0550 and 202/06/0419).

References

1. Winslow W.M., Induced fibrillation of suspension, *J. Appl. Phys.* **20** (1949) pp. 1137–1140.
2. Parthasarathy M. and Klingberg D.J., Electrorheology: mechanisms and models, *Mater. Sci. Eng. R* **17** (1996) pp. 57–103.
3. Hao T., Electrorheological fluids, *Adv. Mater.* **13** (2001) pp. 1847–1857.
4. Hao T., Electrorheological suspensions, *Adv. Colloid Interface Sci.* **97** (2002) pp. 1–35.
5. Henley S. and Filisko F.E., Flow profiles of electrorheological suspensions: An alternative model for ER activity, *J. Rheol.* **43** (1999) pp.1323–1336.
6. Filisko F. E., Henley S. and Quist G., Recent developments in the properties and composition of electrorheological fluids, *J. Intelligent Mater. Syst. Struct.* **10** (1999) pp. 476–480.
7. Wolfram, S., *The Mathematica book*, 3rd ed., Cambridge, New York: Cambridge University Press (1996)
8. Schulz T. J. and Voelz G. D., Signal recovery from autocorrelation and cross-correlation data, *J. of the Optical Society of America A*, **22** (2005) pp. 616-624
9. Liu J. and Iskander M., Adaptive Cross Correlation for Imaging Displacements in Soils, *J. of Computing in Civil Engineering*, **18** (2004) pp. 46-57